A Study of the Ion–Molecule Reactions of the $Cr(CO)_5^-$ Anion with Oxygen

D. L. Bricker and D. H. Russell*

Contribution from the Department of Chemistry, Texas A&M University, College Station, Texas 77843. *Received June 23, 1986*

Abstract: The ion–molecule reactions of the $Cr(CO)_5^-$ anion with molecular oxygen are described. The $Cr(CO)_5^-$ anion reacts with O_2 to produce the $Cr(CO)_3O_2^-$ and $Cr(CO)_3O^-$ anions. The $Cr(CO)_3O_2^-$ anion reacts with neutral $Cr(CO)_6$ to reform $Cr(CO)_5^-$; whereas, the $Cr(CO)_3O^-$ anion reacts with O_2 to form CrO_3^-. The rate of reaction of $Cr(CO)_5^-$ shows an unusual temperature dependence. The temperature-dependent reaction rate is attributed to the formation of a high-spin state of $Cr(CO)_5$ by thermal decomposition of $Cr(CO)_6$. The mechanism of the reaction of $Cr(CO)_5^-$ with oxygen is probed by ($^{18}O_2$) isotopic labeling. The proton and electron affinities of the $Cr(CO)_3O_2^-$, $Cr(CO)_3O^-$, and CrO_3^- anions are measured by using the bracketing method. In addition, the structures of the various anions are probed by using collision-induced dissociation (CID) methods, and the relative abundance of the CID fragment ions is used to estimate relative ligand binding energies for CO and O_2.

Transition metals play an important role in both organic and inorganic chemistry. Transition metal mediated organic synthesis,[1] catalysis,[2] biomolecular synthesis,[3] and organometallic conductors[4] are all current subjects of intense interest. Owing to the frequency of occurrence and diverse chemistry, the transition-metal oxides are of particular importance. The oxides provide information regarding the stability of oxidation states,[5] corrosion chemistry,[6] flame chemistry,[7] and the oxidation of organics.[8] In spite of the importance of metal oxides, only a relatively few studies on the ion–molecule reaction chemistry of metal oxide anions have been reported. In part this sparsity of information is due to the difficulty in generating metal oxide anions in an apparatus suited for ion–molecule chemistry studies.

Recently Squires reported on the formation of chromium oxides by ion–molecule reactions in a flow afterglow apparatus.[9] In this study the $Cr(CO)_5^-$ (m/z 192) anion was generated by dissociative ionization of $Cr(CO)_6$, thermalized by collisions with bath gas, and allowed to react with molecular oxygen. The major ion–molecule product ions formed by reaction of $Cr(CO)_5^-$ with oxygen are $Cr(CO)_3O^-$ (m/z 152) and $Cr(CO)_3O_2^-$ (m/z 168) with these product ions ultimately giving rise to CrO_x^- (x = 2, 3, 4, 5).

On the basis of these experiments Squires suggested that the CrO_3^- ion (m/z 100) must involve a rare oxidation state or unusual bonding modes of oxygen. However, several authors have reported on the formation of high oxidation state chromium anions, and on the basis of this work, CrO_3^- appears to be the normal product ion formed under a variety of conditions. For example, Franklin reported on the formation of a series of chromium oxides of the type $(CrO_3)_n^-$, where n ranges from 1 to 5.[10] In Franklin's experiment, the CrO_3^- anion was generated by sublimation of solid CrO_3 from a Knudsen cell followed by electron impact ionization in the source of a mass spectrometer. Franklin used this method to determine the appearance energies and electron affinities for a series of $(CrO_3)_n$ species. Miller also reported on the formation of CrO_3^- in flame chemistry,[7] and Rudny has reported on the formation of CrO_3^- anions in the gas phase by heterolytic dissociation of potassium chromate.[11]

In related work, Beauchamp studied the dissociative electron attachment reactions of several transition-metal carbonyls[12] including $Cr(CO)_6$. Beauchamp reported a rate for electron attachment to $Cr(CO)_6$ of 3.2×10^{-7} cm^3 molecules^{-1} s^{-1}. The high rate for electron attachment to transition-metal carbonyls makes it possible to study the chemistry of these systems under the low pressures required by ICR. An additional benefit of the high electron capture rate for transition-metal carbonyls is that further reactions of the $Cr(CO)_5^-$ ions are not limited by their rate of formation.

Owing to the importance of transition-metal oxides to many areas of chemistry, we have investigated the chemistry of a number of transition-metal ions and cluster ions with molecular oxygen.[13] This paper deals specifically with the chemistry of $Cr(CO)_5^-$ with O_2. These studies provide thermochemical data, e.g., proton and electron affinities, acid dissociation energies, and relative Cr–O and Cr–CO bond energies. The results are interpreted as evidence that the oxygen atoms of $Cr(CO)_3(O)_2^-$ are bound to Cr as O_2, rather than oxygen atoms as suggested by Squires. Also, a strong temperature dependence for the reaction of $Cr(CO)_5^-$ with O_2 is attributed to the formation of a high energy form of $Cr(CO)_5^-$ by thermal decomposition of $Cr(CO)_6$ to $Cr(CO)_5$ followed by electron attachment to produce $Cr(CO)_5^-$.

Experimental Section

The work described here was carried out on a standard Nicolet FTMS-1000 which has been modified as discussed previously.[14] The modifications included increasing the magnetic field strength from 1.9 to 3 T and increasing the ion cell radius from 2.54 to 5.2 cm. The higher magnetic field strength improves ion trapping efficiency and, with the larger ion cell radius (and high magnetic field), ions can be accelerated to keV energies for collision-induced dissociation (CID). The sample was ionized by electron impact (1 V–50 eV ionizing energy) maintaining a constant electron emission current of 100 +/- 10 nA. The ion trapping voltage was constant at 2.5 V.

Ion-ejection techniques were used to mass-select a specific reactant ion.[15-17] The frequencies utilized for performing ion-ejection were selected so as to minimize the translational excitation of the reactant ion.[17,18] In some experiments the translational energy of the reactant ion was varied to obtain information on the energy dependence for the reaction rate. In these experiments the translational energy of the ion excited by applying a radio frequency pulse to the ion cell transmitter plates is estimated by using methods previously discussed by Beau-

(1) Bergman, R. G. *Science* **1984**, *223*, 902.
(2) Shrock, R. R. *Science* **1983**, *219*, 13.
(3) Halpern, J. *Science* **1985**, *227*, 869.
(4) Marks, T. J. *Science* **1985**, *227*, 881.
(5) Cotton, F. A.; Wilkinson, G. *Advanced Inorganic Chemistry*; 4th ed.; Wiley: New York, 1980; pp 483–501.
(6) Brubaker, G. R.; Phipps, Desh J. *Sci. Ind. Res.* **1977**, *36*, 470.
(7) Miller, W. J. *J. Chem. Phys.* **1972**, *57*, 2354.
(8) Sheldon, R. A.; Kochi, J. K. *Metal-Catalyzed Oxidation of Organic Compounds*; Academic Press: New York, 1981; p 121.
(9) Squires, R. R.; Sallans, L.; Lane, K. *J. Am. Chem. Soc.* **1984**, *106*, 2719.
(10) Franklin, J. L.; Wang, J. L.; Margrave, J. L. *J. Inorg. Nucl. Chem.* **1974**, *37*, 1107.
(11) Rudny, E. B.; Sidorov, L. N.; Kuligina, L. A.; Sememov, G. A. *Int. J. Mass Spectrom. Ion Proc.* **1985**, *64*, 95.
(12) Beauchamp, J. L.; George, P. M. *J. Chem. Phys.* **1982**, *76*, 2959.
(13) Fredeen, D. A.; Russell, D. H., unpublished results.
(14) Bricker, D. L.; Adams, T. A.; Russell, D. H. *Anal. chem.* **1983**, *55*, 2417.
(15) Cody, R. B.; Freiser, B. S. *Int. J. Mass Spectrom Ion Phys.* **1982**, *41*, 199.
(16) Cody, R. B.; Freiser, B. S. *Anal. Chem.* **1982**, *54*, 96.
(17) Jacobsen, D. B.; Freiser, B. S. *J. Am. Chem. Soc.* **1983**, *105*, 736.
(18) Anderson, D. A.; Russell, D. H. *J. Am. Chem. Soc.* **1985**, *107*, 3762.

0002-7863/87/1509-3910$01.50/0

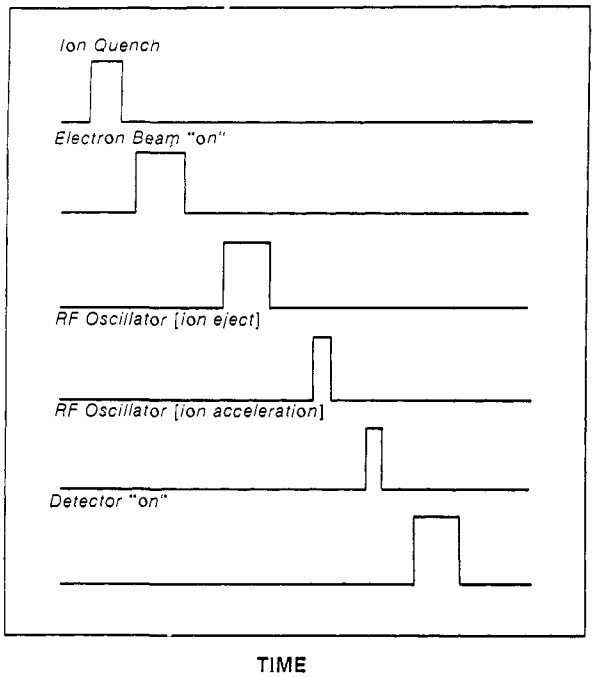

Figure 1. Diagram of pulse sequence used for the Fourier transform mass spectrometry experiments.

champ.[19] However, it should be noted that this method for estimating the translational energy of the ion gives the maximum energy for the ion, rather than an average value for the translational energy. Thus it is not possible to extract absolute energy dependence values from such measurements.

At present our instrument does not have the capabilities to eject electrons, which may effect kinetic measurements. Therefore a set of experiments were conducted to determine the effect of trapped electrons on the reaction rate. After initial formation of the $Cr(CO)_5^-$, the $Cr(CO)_5^-$ was ejected from the cell. A short delay after ejection allowed $Cr(CO)_6$ neutrals in the cell to capture an electron before detection. The time between ionization and ejection was varied until $Cr(CO)_5^-$ was no longer formed after ejection. The time for $Cr(CO)_6$ to scavenge the trapped electrons was approximately 35 ms under the conditions (beam time, emission current, and pressure of the experiments described in this paper. That is, after 35 ms all of the trapped electrons are scavenged by the $Cr(CO)_6$. Since the time for reaction is on the order of 300 ms, trapped electrons produce no more than a 10% error in the measured reaction rates.

A diagram depicting a typical FTICR experimental sequence is shown in Figure 1. The quench pulse removes all ions from the trap cell prior to formation of new ions. The radio frequency oscillators used for ion ejection are swept over the desired mass range following electron impact ionization of the sample. A variable delay time between ion ejection and ion detection is used to control the ion–molecule reaction time and to allow time for collisions during CID experiments.

The kinetics for the ion–molecule reactions of the $Cr(CO)_5^-/O_2$ system were studied by measuring the disappearance of primary ions as a function of time. A plot of ln $[I/I_0]$ vs. reaction time was used to determine the rate constant for reactions 5 and 6. The reaction rate constant is then calculated by using eq 1, where I_0 is the initial signal

$$\ln [I(t)/I_0] = -nkt \qquad (1)$$

intensity for the reactant ion, $I(t)$ is the intensity of the ion at time t, n is the number density of the neutrals,[21] and k is the rate constant. The data were then plotted as ln $[I(t)/I_0]$ vs. t and fitted by using a linear least-squares method to calculate the slope of the line. The rate constant for reaction of $Cr(CO)_5^-$ with O_2 was calculated by dividing the slope of the line by the number density of the reactant neutrals in the cell. The analyzer pressure was monitored with a Granville-Phillips series 280 ionization gauge controller. The density of the neutral reagent was estimated with the ionization gauge following calibration procedures described previously. It should be noted that the major source of errors for the measured rate constants arises from the pressure measurements.

(19) Beauchamp, J. L. *Annu. Rev. Phys. Chem.* **1971**, *22*, 527.
(20) Freiser, B. S.; Carlin, T. J. *Anal. Chem.* **1983**, *55*, 571.
(21) Lehman, T. A.; Bursey, M. M. *Ion Cyclotron Resonance Spectrometry*; Wiley-Interscience: New York, 1976.

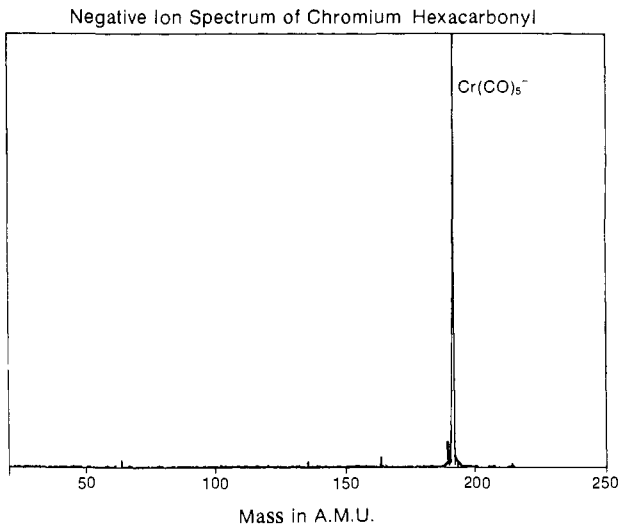

Figure 2. FT mass spectrum of $Cr(CO)_6$. Experimental conditions are given in the text.

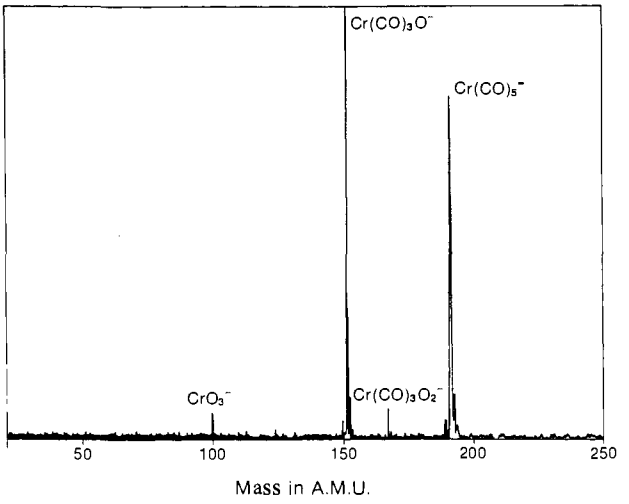

Figure 3. FT mass spectrum of $Cr(CO)_6$ with added O_2. The time delay allowed for $Cr(CO)_5^-$ to react with the O_2 is approximately 500 ms.

All chemicals used in these studies were obtained from standard chemical sources and were used without further purifications. The samples were admitted to the analyzer region by variable leak valves (Varian Model 951-5106). The pressure of each reactant was varied from 5×10^{-8} to 6×10^{-7} Torr. In the special cases of sample introduction by the pulsed valve (General Valve Series 9), the valve was operated by a controller system designed and constructed at TAMU.

Results

Upon electron impact (electron energies between 1 and 50 eV) $Cr(CO)_6$ undergoes dissociative electron capture generating the 17-electron radial anion $Cr(CO)_5^-$ (m/z 192) and neutral carbon monoxide, eq 2[12] (see Figure 2). The fifteen-electron $Cr(CO)_4^-$

$$Cr(CO)_6 + e^- \rightarrow Cr(CO)_5^- + CO \qquad (2)$$

radical anion (m/z 164) is also formed; however, the relative abundance of this ion is less than 15%. In addition, the $Cr(CO)_4^-$ anion (m/z 164) readily reacts with $Cr(CO)_6$ either by simple charge transfer (reaction 3) or by ligand extraction (reaction 4) to generate the $Cr(CO)_5^-$ anion (m/z 192). In either case $Cr(CO)_5^-$ (m/z 192) is the observed product ion formed by reaction of $Cr(CO)_4^-$ with $Cr(CO)_6$.

$$Cr(CO)_4^- + Cr(CO)_6 \rightarrow Cr(CO)_4 + Cr(CO)_5^- + CO \qquad (3)$$

$$Cr(CO)_4^- + Cr(CO)_6 \rightarrow Cr(CO)_5^- + Cr(CO)_5 \qquad (4)$$

The chromium pentacarbonyl anion, $Cr(CO)_5^-$ (m/z 192), readily reacts with molecular oxygen to form two primary product ions, $Cr(CO)_3O_2^-$ (m/z 168) and $Cr(CO)_3O^-$ (m/z 152) anions

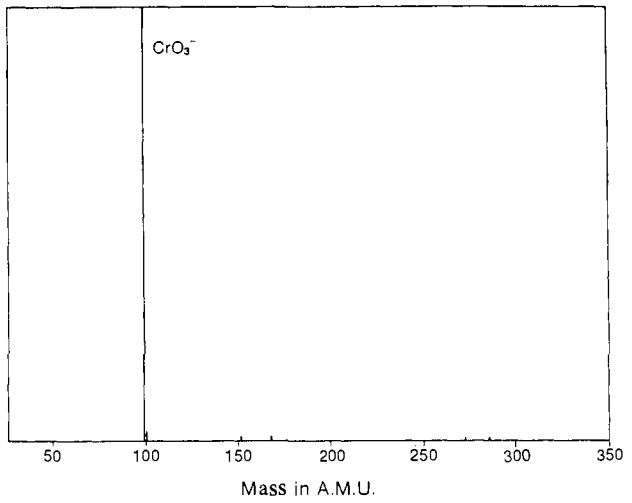

Figure 4. Same mass spectrum as given in Figure 3 except the ion–molecule reaction time has been increased to 1.5 s.

(eq 5 and 6) (Figure 3).[9] The ratio of the product ions is sensitive to both pressure of $Cr(CO)_6$ and translational energy of the $Cr(CO)_5^-$ anion (m/z 192). The $Cr(CO)_3O_2^-$ anion (m/z 168) undergoes dissociative charge transfer reaction with neutral $Cr(CO)_6$ to regenerate the $Cr(CO)_5^-$ anion (m/z 192) (eq 7), whereas the $Cr(CO)_3O^-$ anion (m/z 152) reacts with an additional molecule of oxygen to yield the CrO_3^- anion (m/z 100) (eq 8). The CrO_3^- (m/z 100) anion is the final product ion formed up to reaction times of several seconds (see Figure 4).

$$Cr(CO)_5^- + O_2 \begin{cases} \rightarrow Cr(CO)_3O_2^- + 2CO & (5) \\ \rightarrow Cr(CO)_3O^- + CO + CO_2 & (6) \end{cases}$$

$$Cr(CO)_3O_2^- + Cr(CO)_6 \rightarrow Cr(CO)_5^- \quad (7)$$

$$Cr(CO)_3O^- + O_2 \rightarrow CrO_3^- + 3CO \quad (8)$$

The sequence of ion–molecule reactions for the $Cr(CO)_5^-/O_2$ system was studied by using three experimental methods. The first method involved ion ejection.[15] After ionization of the $Cr(CO)_6$, the $Cr(CO)_5^-$ anion (m/z 192) was allowed to react with molecular oxygen to produce $Cr(CO)_3O_2^-$ and $Cr(CO)_3O^-$ (m/z 152). The $Cr(CO)_5^-$ and $Cr(CO)_3O_2^-$ anions were then ejected from the ion cell, leaving only $Cr(CO)_3O^-$ ions in the ion cell. The $Cr(CO)_3O^-$ anion reacts with molecular oxygen to produce the CrO_3^- anion (m/z 100) (eq 8) and with residual $Cr(CO)_6$ in a dissociation charge transfer or ligand abstraction reaction (eq 9 and 10) to regenerate the $Cr(CO)_5^-$ radical anion (m/z 192).

$$Cr(CO)_3O^- + Cr(CO)_6 \begin{cases} \rightarrow Cr(CO)_5^- + Cr(CO)_3O + CO & (9) \\ \rightarrow Cr(CO)_5^- + Cr(CO)_4O & (10) \end{cases}$$

The same ion ejection procedure was used to study the ion–molecule reactions of the $Cr(CO)_3O_2^-$ anion (m/z 168). The $Cr(CO)_3O_2^-$ anion does not react with molecular oxygen, but it does undergo charge transfer or ligand abstraction reactions with residual $Cr(CO)_6$ to regenerate the $Cr(CO)_5^-$ anion (eq 11 and 12). It was not necessary to use ion ejection to study the CrO_3^- anion (m/z 192). The CrO_3^- anion (m/z 100) is the terminal ion formed at all pressures of reactants employed and remained the only ion observed in the spectrum for reaction times up to several seconds.

$$Cr(CO)_3O_2^- + Cr(CO)_6 \begin{cases} \rightarrow Cr(CO)_5^- + Cr(CO)_3O_2 + CO & (11) \\ \rightarrow Cr(CO)_5^- + Cr(CO)_4O_2 & (12) \end{cases}$$

The second method used to examine the $Cr(CO)_5^-/O_2$ system involved the use of a pulsed valve for sample introduction. The methodology for pulsed valve sample introduction has been described by Freiser.[20] The major advantage for using pulsed valves is to permit introduction of the sample at a specific point in the reaction sequences (see Figure 1). In one set of experiments, the oxygen pressure in the analyzer was maintained constant and

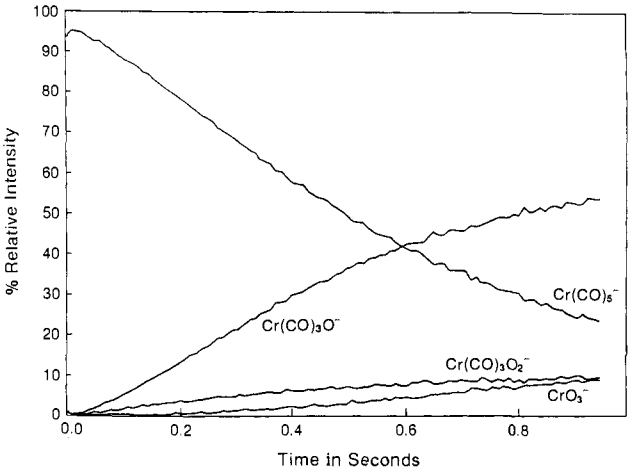

Figure 5. Temporal plot for the ion–molecule reaction data for $Cr(CO)_5^-$ reacting with O_2. The sample inlet temperature is maintained at ca. 25 °C.

$Cr(CO)_6$ was admitted to the analyzer via the pulsed valve. The $Cr(CO)_6$ reagent was admitted to the analyzer prior to the ionization step (Figure 1). Following ionization, the $Cr(CO)_5^-$ anion (m/z 192) was allowed to react with molecular oxygen in the normal reaction sequence. The advantage of this approach is that the residual $Cr(CO)_6$ is pumped away, eliminating competing reactions (e.g., reactions 7 and 9–12). The $Cr(CO)_3O^-$ anion (m/z 152) formed by reaction 6 was ejected from the cell leaving only the $Cr(CO)_3O_2^-$ anion (m/z 168). The $Cr(CO)_3O_2^-$ anion (m/z 168) remained as the only ion in the spectrum up to reaction times of several seconds. The results of the experiment indicate that the $Cr(CO)_3O_2^-$ anion (m/z 168) does not react with oxygen and is stable, i.e., does not decompose on the time scale of several seconds to yield $Cr(CO)_3O^-$ (m/z 152).

The third method used to study the reaction sequence of the $Cr(CO)_5^-/O_2$ system involved the use of isotopic labeling [$^{18}O_2$] in combination with pulsed valve sample introduction and ion-ejection. The pulsed valve was used to introduce $Cr(CO)_6$ prior to pulsing the electron beam. The $Cr(CO)_5^-$ anion (m/z 192) was then allowed to react with $^{18}O_2$, resulting in the formation of $Cr(CO)_3{}^{18}O_2^-$ and $Cr(CO)_3{}^{18}O^-$ (eq 13 and 14). In this

$$Cr(CO)_5^- + {}^{18}O_2 \begin{cases} \rightarrow Cr(CO)_3{}^{18}O_2 + 2CO & (13) \\ \rightarrow Cr(CO)_3{}^{18}O^- + CO + CO_2 & (14) \end{cases}$$

experiment, the mass of the $Cr(CO)_3O^-$ anion shifted from m/z 152 to m/z 154, the mass of the $Cr(CO)_3O_2^-$ anion shifted from m/z 168 to m/z 172, and the mass of the CrO_3^- anion shifted from m/z 100 to m/z 106. This experiment demonstrates that scission of the C–O bond in the bound carbonyl ligands does not occur and that reaction 6 involves addition of O_2 to $Cr(CO)_5^-$ followed by elmination of the elements CO plus CO_2.[9] Likewise, O_2 addition to $Cr(CO)_3O^-$ involves elimination of the elements 3CO, i.e., the reaction is a simple ligand exchange reaction.

A particular anomaly of the $Cr(CO)_5^-/O_2$ system is that the reaction rate increases by an order of magnitude when the sample inlets are heated to ca. 100 °C. For instance, at ambient temperature (22 °C) [molecular oxygen pressure of 4×10^{-7} torr and $Cr(CO)_6$ pressure of 2×10^{-7} torr] the relative abundance of the $Cr(CO)_3O^-$ anion (m/z 152) reaches 100% relative intensity at a reaction time of approximately 600 ms (see Figure 5); whereas, at elevated temperatures (e.g., 100 °C) [identical $Cr(CO)_6$ and O_2 pressures] the same extent of conversion to product ions requires less than 300 ms (Figure 6). The reaction was repeated several times at various pressures of the reactants and in all cases the reaction proceeds significantly faster (by an order of magnitude) with a hot inlet vs. a cold inlet. The design of the present inlet system does not allow separate heating of the individual reagent inlets.

Such a strong temperature dependence for an ion–molecule reaction is rather unusual and suggests that the reaction involves

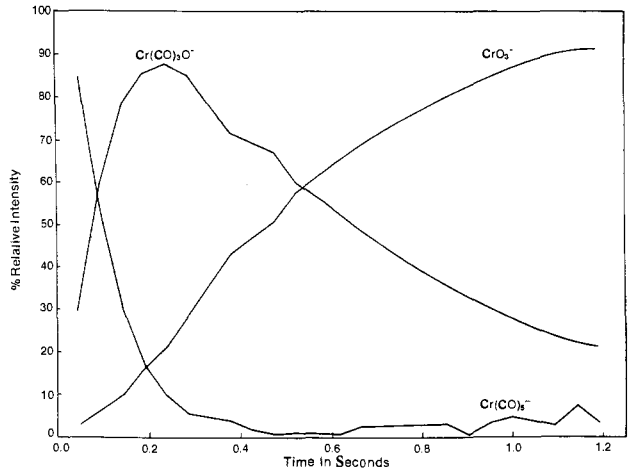

Figure 6. Same data as in Figure 5 except the sample inlet temperature has been increased to ca. 100 °C.

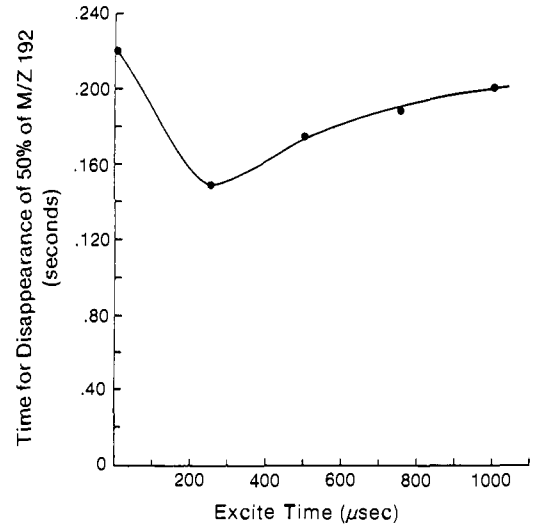

Figure 7. A plot of the ion–molecule reaction time required for 50% of the $Cr(CO)_5^-$ ions to react with O_2 as the translational energy of the anion is increased (see Experimental Section).

a novel potential energy surface or that the reaction is state (structure) specific. In an effort to elucidate the temperature dependence for reactions 5 and 6 several methods were employed to produce excited $Cr(CO)_5^-$ anions. First, $Cr(CO)_5^-$ was formed at different ionizing energies (ca. 1 to 50 eV) and the rate of disappearance of the $Cr(CO)_5^-$ was measured. To a first approximation (+/− 10%) the rate of disappearance of $Cr(CO)_5^-$ is independent of the initial ionizing energy. Second, studies were performed on translationally excited $Cr(CO)_5^-$ anions. The ions were excited translationally by applying a radio-frequency pulse at a frequency "on" resonance with m/z 192 (239.8 KHz).[16,17] We chose to use "on-resonance" excitation vis-ā-vis "off-resonance"[17] excitation in order to better estimate the maximum translational energy of the ions after excitation (see Experimental Section). The rate of disappearance of the $Cr(CO)_5^-$ anion (m/z 192) with O_2 increases with increasing translational energy. The rate of disappearance of $Cr(CO)_5^-$ reaches a maximum when the radio-frequency pulse is applied for 200 ms (Figure 7); the maximum translational energy acquired by the $Cr(CO)_5^-$ anion (m/z 192) under these conditions is approximately 2 eV or 45 kcal/mol (laboratory frame: 1.7 eV center-of-mass energy).[16,19] It should be noted, however, that the rate of reaction changes by only a factor of ca. 1.5.

A separate series of experiments have been conducted in an attempt to understand the anomalous temperature dependence. The proton and electron affinities of the $Cr(CO)_5^-$ and the two primary product ions (e.g., $Cr(CO)_3O_2^-$ and $Cr(CO)_3O^-$) were measured as a function of the inlet temperature. Although one might expect a detectable difference in the proton and electron affinities if an excited state of $Cr(CO)_5^-$ is responsible for the increased reactivity, the data did not change within the resolution of the experiment. Also CID spectra of the ions are the same for "hot" and "cold" inlets, thus we cannot attribute the effects to structural difference in the product ions. The relative abundance of the fragment ions in the CID spectra did not change more than 5% for "hot" vs. "cold" inlets. Although a detailed understanding of the temperature dependence for the reaction is not available, it is clear that the internal energy of the $Cr(CO)_5^-$ is an important factor.

Table I. Kinetics Data for the $Cr(CO)_5^-/O_2$ Ion–Molecule Chemistry

condition	rate[a]	efficiency
constant P/ambient T	1.54×10^{-10}	0.22
constant P/hot inlet	1.54×10^{-9}	2.8
constant P/rf applied[b]	3.97×10^{-10}	0.71
squires	3.95×10^{-11}	0.05

[a] The error in the rate measurement is +/− 10% due to the relative error of the ionization guage. The units are cm^3 $molecule^{-1}$ s^{-1}. [b] The rate constant for this measurement was obtained at the maximum rate from Figure 7.

Using similar experimental methods, the translational energy dependence for the reaction of $Cr(CO)_3O^-$ (m/z 152) with molecular oxygen was studied. Translational excitation of the $Cr(CO)_3O^-$ anion (m/z 152) increases the rate of reaction of $Cr(CO)_3O^-$ anion (m/z 152) with molecular oxygen by a factor of 3. The rate of reaction reaches a maximum at a maximum translational energy of 10 eV (230 kcal/mol, 8.3 eV center-of-mass). (The relative error in the estimated translational energy is +/− 25%.)[19] For comparison these data are also included in Table I.

The efficiency for the $Cr(CO)_5^-/O_2$ reaction was estimated by comparing k_{obsd} to $k_{Langevin}$ (see Table I).[22] For comparison, the kinetic results of Squires[9] are also given in Table I. An important point to note from Table I is the dramatic increase in k with a heated inlet and when the $Cr(CO)_5^-$ ion is translationally excited.

Smith and Adams[23] have noted differences in the measured rate constants of ion–molecule reactions when measured in the flowing afterglow and ICR. They attribute the difference to the collision-dominated environment of the flowing afterglow and collision-free environment of the ICR. Also, excess internal energy remaining in the ion following ionization is removed by collisional deactivation in the flowing afterglow, whereas the number of stabilizing collisions is greatly reduced in the ICR experiment.

Proton and Electron Affinity Measurements. Thermochemical data, e.g., proton affinities and electron affinities, for gas-phase molecular ions can be obtained by using the methods developed by Bartmess and McIver[24] and Bowers.[25]

The proton affinities of all three chromium oxides studied, e.g., $Cr(CO)_3O^-$ (m/z 152), $Cr(CO)_3O_2^-$ (m/z 168), and CrO_3^- (m/z 100), are bracketed by acetic acid (proton affinity 348 kcal/mol) and phenol (proton affinity 350 kcal/mol). These measurements yield a proton affinity for all three oxides of 349 +/− 1 kcal/mol. There are no known literature values to compare with these results.

(22) Bartmess, J. E.; McIver, R. T. In *Gas Phase Ion Chemistry*; Bowers, M. T., Ed.; Academic Press: New York, 1979; Vol. 2.
(23) Smith, D.; Adams, N. G. In *Gas Phase Ion Chemistry*; Bowers, M. T., Ed.; Academic Press: New York, 1979; Vol. 1.
(24) Bartmess, J. E.; Scott, J. P.; McIver, R. T. *J. Am. Chem. Soc.* **1979**, *101*, 6040.
(25) Aue, D. H.; Webb, H. M.; Bowers, M. T. *J. Am. Chem. Soc.* **1976**, *98*, 311.
(26) Armentrout, P. B.; Halle, L. F.; Beauchamp, J. L. *J. Am. Chem. Soc.* **1981**, *103*, 6501.
(27) Armentrout, P. B.; Halle, L. F.; Beauchamp, J. L. *J. Chem. Phys.* **1982**, *76*, 2444.
(28) Patai, S. *The Chemistry of Peroxides*; John Wiley and Sons: New York, 1982; p 469.
(29) Miller, M. T. *NBS Spec. Publ. (U.S.)* **1979**, No. 56111, 443.
(30) Janousek, B. K.; Brauman, J. I. In *Gas Phase Ion Chemistry*; Bowers, M. T., Ed.; Academic Press: New York, 1979; Vol. 2, pp 53–86.
(31) Schilling, J. B.; Goddard, W. A.; Beauchamp, J. L. *J. Am. Chem. Soc.* **1986**, *108*, 582.

Table II. Data for Chromium Oxide Collision-Induced Dissociation Anions

precursor	fragment Ions (relative abundance)
$Cr(CO)_3O_2^-$	$Cr(CO)_3^-$ (42); $Cr(CO)_2^-$ (10)[a]
	$Cr(CO)_3^-$ (100); $Cr(CO)_2^-$ (43); Cr^- (24)[b]
$Cr(CO)_3O^-$	$Cr(CO)_2O^-$ (100); $Cr(CO)O^-$ (57); CrO^- (21)[b]
CrO_3^-	CrO_2^- (27); CrO^- (18); Cr^- (10)[b]

[a] The translational energy of the anions was approximately 20 eV. [b] The translational energy of the anions was approximately 200 eV.

The electron affinity of $Cr(CO)_6$ cannot be directly determined in this experiment since it undergoes a dissociative electron capture and the $Cr(CO)_6^-$ radical anion is not observed. Sallans[32] has reported an electron affinity value of 2.3 eV (52.2 kcal/mol) for $Cr(CO)_5$.

The electron affinities of $Cr(CO)_3O$ and $Cr(CO)_3O_2$ were also determined by the bracketing method. The electron affinity for both species is bracketed on the upper end by $Cr(CO)_5$ (EA 2.3 eV)[33] and on the lower end by NO_2 (EA 2.2 eV).[33] This gives a value of 2.2 +/- 0.1 eV for the electron affinity of $Cr(CO)_3O$ and $Cr(CO)_3O_2$. The electron affinity of CrO_3 is bracketed by chloranil (2.7 eV) and $Cr(CO)_5$ (2.3 eV). These measurements provide an electron affinity of 2.5 +/- 0.2 eV for CrO_3. For comparison, Miller[7] has reported a value for the electron affinity of CrO_3 of 2.4 +/- 0.5 eV.

Collision-Induced Dissociation (CID) Studies. Collision-induced dissociation (CID) spectra were obtained for the $Cr(CO)_3O_2^-$ (m/z 168), $Cr(CO)_3O^-$ (m/z 152), and CrO_3^- (m/z 100) anions. The results of the CID spectra are tabulated in Table II. Upon collisional activation the $Cr(CO)_3O_2^-$ anion (m/z 168) readily loses 32 mass units, i.e., O_2, which suggests the binding energy of O_2 is less than that for CO. Note also the absence of a signal in the CID spectrum for loss of O to give $Cr(CO)_3O^-$ (m/z 152). Increasing the translational energy (see Experimental Section) at which collisional activation is performed results in an increase in the relative abundance of the CID fragment ions corresponding to loss of multiple CO ligands (Table II).

The data from the CID of $Cr(CO)_3O^-$ (m/z 152) are also given in Table II. In contrast to $Cr(CO)_3O_2^-$ (m/z 168), the carbonyl ligands of $Cr(CO)_3O^-$ (m/z 152) are more weakly bound than the oxygen atom, e.g., the dominant CID product ions correspond to loss of CO and 2CO and loss of O is not observed. Gradual increases in the translational energy of the CrO_3^- ion (m/z 100) result in successive loss of oxygen atoms. We interpret the CID data for CrO_3^- as evidence that the oxygens are bound as single atoms to Cr as opposed to molecular oxygen.

Discussion

The temperature and translational energy dependence for the $Cr(CO)_5^-/O_2$ reaction can be attributed to two factors. (i) Reactions 5 and 6 are endothermic; however, as Squires[9] has pointed out and thermodynamic calculations suggest, the reaction should be exothermic.[27,28] (ii) The overall reaction is exothermic, but the reaction is subject to an energy barrier.

A more realistic explanation for the temperature dependence of the reaction rate is to invoke a change in the energy or structure of the reactant $Cr(CO)_5^-$ anion. It has been assumed throughout the previous discussion that the neutral $Cr(CO)_6$ reaches the cell region intact and dissociative electron attachment involves electron capture and expulsion of a carbonyl ligand. Any excess internal energy imparted to the molecule upon ionization is converted into vibrational or translational energy of the ion and neutral. By such a process the $Cr(CO)_5^-$ anion (m/z 192) would remain in the thermodynamically favored octahedral structure. However, the decomposition point for $Cr(CO)_6$ is 110 °C and this decomposition may be facilitated by the stainless steel inlet system. Therefore, $Cr(CO)_5$ formed by thermal decomposition of $Cr(CO)_6$ reaches the cell and upon ionization (electron capture) excess energy cannot be removed by the displaced CO ligand.

A referee has pointed out an alternative suggestion to the increased rate of reaction. He suggests that the internal energy of the $Cr(CO)_6$ at 100 °C facilitates dissociative attachment with the excess internal energy remaining in the $Cr(CO)_5^-$. In either case $Cr(CO)_5^-$ is vibrationally excited and the reaction of $Cr(CO)_5^-$ with O_2 is vibrationally driven. The excess internal energy of the $Cr(CO)_5^-$ anion (m/z 192) serves to increase the reaction efficiency by providing the energy necessary to overcome an energy barrier to product formation. This mechanism is consistent with the increase in the rate constant for product formation with temperature (inlet) and translational energy of the $Cr(CO)_5^-$ anion. That is, the most probable consequence of translationally exciting $Cr(CO)_5^-$ is collisional activation to produce a vibrationally excited $[Cr(CO)_5^-]^*$ anion.

Information on the structure and ligand binding energies for the $Cr(CO)_3O^-$ and $Cr(CO)_3O_2^-$ anions comes from the CID results. On the basis of relative abundance of the fragment ions, the CID spectra for the $Cr(CO)_3O_2^-$ anion suggest that the O_2 ligand is bound more weakly than the carbonyl ligands. Conversely, for the $Cr(CO)_3O^-$ anion, the binding energy of the oxygen atom is greater than that for the carbonyl ligands (see Table II). From the CID results it may be assumed that the oxygen–oxygen bond in the $Cr(CO)_3O_2^-$ anion is stronger than the chromium–oxygen bond since loss of molecular oxygen rather than an oxygen atom is observed in the CID spectrum. Two plausible structures for $Cr(CO)_3O_2^-$ are I and II. Both of these structures are consistent with the fragment ions observed in the CID spectrum, i.e., loss of the O_2 ligand would produce the $Cr(CO)_3^-$ anion. However, in structure I the O_2 ligand is bound as a "peroxo" oxygen and one would expect a stronger ligand binding energy (relative to structure II) for such a structure.[27] Furthermore, formation of a structure such as I involves electron donation from the metal to the antibonding oxygen orbitals ($1\Sigma_u^*$) which lowers the O---O dissociation energy,[27] possibly resulting in loss of O (or loss of CO_2 analogous to reaction 6) from $Cr(CO)_3O_2^-$ to be competitive with loss of O_2.

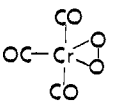

I

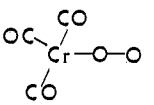

II

The electron affinities for the chromium oxides increase as the number of bound oxygen increases. For instance, the electron affinities for Cr, CrO, CrO_2, and CrO_3 are 0.67 +/- 0.1, 1.4 +/- 0.4, 2.1 +/- 0.7, and 2.4 +/- 0.4 eV, respectively,[29] whereas, the electron affinities for $Cr(CO)_3O$ and $Cr(CO)_3O_2$ are 2.2 +/- 0.2 eV. It is interesting to note that the electron affinities of $Cr(CO)_3O$ and $Cr(CO)_3O_2$ are roughly the same as the electron affinity of CrO_2. The constant electron affinities for CrO_2, $Cr(CO)_3O$, and $Cr(CO)_3O_2$ suggest that (i) the carbonyl ligands have the same effect on the electron affinity as oxygen and (ii) that the negative charge on $Cr(CO)_3O$ and $Cr(CO)_3O_2$ resides (predominantly) on the Cr atom, i.e., the electron is localized on the Cr atom.

McIver and Bartmess have pointed out previously that relative acidities of gas-phase ions are an effect based solely on intrinsic structural differences of the ions.[24] With use of a thermochemical cycle and the thermochemical data obtained in these experiments, the bond dissociation energy of the acids may be calculated by using eq 15. For these calculations a value of 313.6 kcal mol^{-1} is used for the ionization energy of $H^\bullet$ [IE(H)], and H_f(acid) is obtained from the proton affinity measurements, e.g., $H_f = -PA$.[31]

$$D(A\text{–}H) = H_{acid} - IE(H) + EA(A) \qquad (15)$$

The value obtained for $D(CrO_3\text{---}H)$ is 94.0 +/- 10 kcal/mol. Similarly, the values for $Cr(CO)_3O^-$ and $Cr(CO)_3O_2^-$ are 86.0 +/- 10 kcal/mol. The thermochemical data for the chromium oxides are summarized in Table III.

The homolytic bond dissociation energies obtained for $Cr(CO)_3OH$, CrO_3H, and $Cr(CO)_3O_2H$ differ substantially from that for $[Cr(CO)_6H]^+$.[31] However, examination of the homolytic bond

(32) Stevens, A. E.; Beauchamp, J. L. *J. Am. Chem. Soc.* **1981**, *103*, 190.
(33) Sallans, L.; Lane, K. R.; Squires, R. R.; Freiser, B. S. *J. Am. Chem. Soc.* **1985**, *107*, 4379.

Table III. Thermochemical Data for the Chromium Oxides

oxide	EA (eV)	PA (kcal/mol)	DH(A–H) kcal/mol
$Cr(CO)_3O$	2.2 +/- 0.2	349 +/- 1	86.0 +/- 10
$Cr(CO)_3O_2$	2.2 +/- 0.2	349 +/- 1	86.0 +/- 10
CrO_3	2.5 +/- 0.2	349 +/- 1	94.0 +/- 10

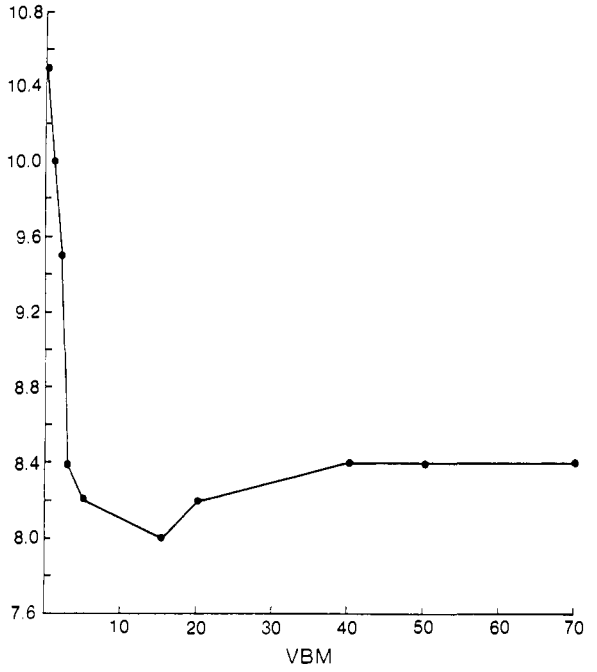

Figure 8. A plot of the $Cr(CO)_3O^-/Cr(CO)_3O_2^-$ ratio as a function of the energy of the ionizing electrons.

dissociation energy data for a series of Cr species reveals an interesting trend, viz., the homolytic bond dissociation energy increases as the electron density of the metal center increases. For example, $D(Cr^+\text{---}H)$ = 31 kcal mol^{-1},[32] $D(Cr\text{---}H)$ = 41.2 kcal mol^{-1},[33] and $D(Cr(CO)_6^+\text{---}H)$ = 58.2 kcal mol^{-1}.[31] The implications of these results are presently being investigated further. However, on the basis of homolytic bond dissociation energies it appears that the electron densities around the Cr atom in $Cr(CO)_3O^-$ and $Cr(CO)_3O_2^-$ are greater than $D(Cr(CO)_6^+\text{---}H)$.[31] This could indicate a formal oxidation state for Cr in $Cr(CO)_3O^-$ and $Cr(CO)_3O_2^-$ of 0, e.g., in each case the ligands being O^- and O_2^-, respectively. Thus the larger values of $D(M\text{---}H)$ for both $Cr(CO)_3OH$ and $Cr(CO)_3O_2H$ are consistent with Beauchamp's idea that "compounds with higher oxidation states of the same metal atom have substantially weaker metal–hydrogen bonds".[31]

Mechanism for Reaction of $Cr(CO)_5^-$ with O_2. Shown in Figure 8 is the ratio for $Cr(CO)_3O^-/Cr(CO)_3O_2^-$ as a function of the initial ionizing energy, and Figure 9 displays the ratio for $Cr(CO)_3O^-/Cr(CO)_3O_2^-$ as a function of translational energy of the $Cr(CO)_5^-$. Note that the relative abundance of $Cr(CO)_3O^-$ decreases under conditions where $Cr(CO)_5^-$ is formed with excess internal energy, e.g., as the ionizing electron energy is increased, and when $Cr(CO)_5^-$ is translationally excited. Also, the relative abundance of $Cr(CO)_3O_2^-$ increases from ca. 10% to ca. 17–18% when the inlet system temperature is increased from ambient to 100 °C. These data suggest that as the internal energy of the reactant $Cr(CO)_5^-$ ion is increased the formation of $Cr(CO)_3O_2^-$ becomes more favored. For thermal or low-energy ions the lifetime of the collision complex decreases exponentially with increasing translational energy.[34] Likewise the lifetime of the collision complex decreases with increasing internal energy of the reactant ions/neutrals. Owing to the decrease in the ratio of the $Cr(CO)_3O^-/Cr(CO)_3O_2^-$ with increasing energy of the collision complex it is proposed that the $Cr(CO)_3O_2^-$ anion is the kinetically

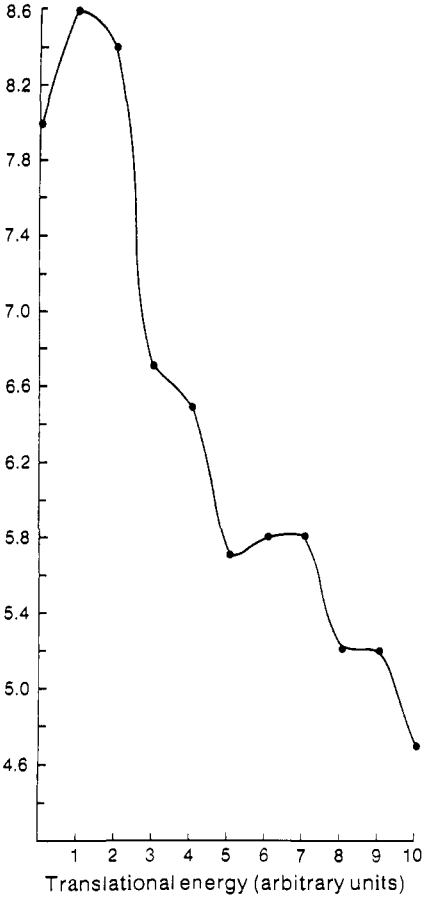

Figure 9. A plot of the $Cr(CO)_3O^-/Cr(CO)_3O_2^-$ ratio as a function of the relative translational energy of the $Cr(CO)_5^-$ anion.

Scheme I

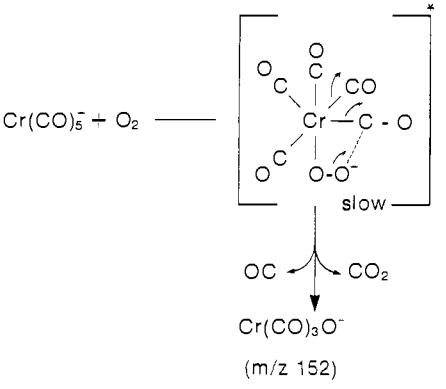

favored product and the $Cr(CO)_3O^-$ anion is the thermodynamically favored product. That is, formation of $Cr(CO)_3O_2^-$ involves simple ligand exchange, i.e., addition of O_2 followed by the elimination of 2CO, whereas, formation of $Cr(CO)_3O^-$ must involve a rearrangement or isomerization process with elimination of CO_2 and CO (Scheme I). Although there have not been any detailed studies on the elimination of CO_2 (or C_2O by CID) from ionized transition-metal carbonyls, preliminary work in our laboratory suggests that such reactions increase in importance as the metal-to-ligand ratio approaches unity.[35] In these coordinatively unsaturated metal ions and/or ionic cluster fragments the ligands are polarized to the extent that multiple ligand metal interactions become possible, and in some cases the carbonyl ligand acts as a 4-electron rather than a 2-electron donor.[36] For ligands more

(34) Dawson, P. H.; Douglas, D. J. *Int. J. Mass Spectrom. Ion Phys.* **1983**, *47*, 121.

(35) Tecklenburg, R. T.; Russell, D. H. *J. Inorg. Chem.*, manuscript to be submitted.

(36) (a) Anderson, D.; Russell, D. H. *J. Am. Chem. Soc.* **1985**, *107*, 3762. (b) Fredeen, D. A.; Russell, D. H. *J. Am. Chem. Soc.* **1986**, *108*, 1860.

strongly polarized than CO, e.g., O_2, such interactions could serve to catalyze rearrangement of the ligands such as proposed in Scheme I.

Conclusions

In this paper it is proposed that the ion–molecule reaction between $Cr(CO)_5^-$ and O_2 to produce $Cr(CO)_3O_2^-$ and $Cr(CO)_3O^-$ occurs by a competitive reaction mechanism. The two mechanisms involve (i) simple ligand exchange to produce the $Cr(CO)_3O_2^-$ anion and (ii) addition of O_2 to $Cr(CO)_5^-$ followed by intramolecular nucleophilic addition of O^- to a CO ligand to form $Cr(CO)_3O^-$ and CO plus CO_2.

A surprisingly large temperature dependence for the rate of reaction of $Cr(CO)_5^-$ with O_2 is observed. The strong temperature dependence of the reaction rate is attributed to formation of a high-energy $[Cr(CO)_5^-]^*$ species. The high-energy $Cr(CO)_5^-$ anion may be formed by thermal decomposition of $Cr(CO)_6$ to give a high spin state of $Cr(CO)_5$, which is subsequently ionized by electron attachment to give $[Cr(CO)_5^-]^*$.

A particularly important result of this study is the proton and electron affinity data obtained for $Cr(CO)_3O^-$ and $Cr(CO)_3O_2^-$. Although the oxygen ligand in these two ions differs significantly, the fact that both ions have the same proton and electron affinities suggests that the oxygen atom and molecule interact with the $Cr(CO)_3$ moiety in an analogous manner. We propose that in both $Cr(CO)_3O^-$ and $Cr(CO)_3O_2^-$ the Cr atom is best described as a Cr° oxidation state and the oxygen ligand as O^- and O_2^-, respectively. These results suggest that proton and electron affinity data may be extremely useful as diagnostic tools for probing the electronic environment of metal centers in gas-phase organometallic systems. A similar suggestion has been reported by Squires on the interplay between electron and proton affinities of metal atoms and ions.[37]

Acknowledgment. This research is supported by the U. S. Department of Energy, Office of Basic Energy Sciences (DE-FG05-85ER13434). The FTMS-1000 system was purchased from funds provided by the Texas A&M University Center for Energy and Mineral Resources, Office of University Research, and Texas Agriculture Experiment Station.

(37) Squires, R. R. *J. Am. Chem. Soc.* **1985**, *107*, 4385.

A Parallel Right-Handed Duplex of the Hexamer d(TpTpTpTpTpT) with Phosphate Triester Linkages

Leo H. Koole,* Marcel H. P. van Genderen, and Hendrik M. Buck

Contribution from The Department of Organic Chemistry, Eindhoven University of Technology, 5600 MB Eindhoven, The Netherlands. *Received November 3, 1986*

Abstract: We show in this work that stable parallel thymine–thymine (T–T) base pairs can be formed in aqueous solution. Initially, this observation was made with 3′,5′-di-*O*-acetylthymidine in water which showed an imino resonance at 13.45 ppm in the ^1H NMR spectrum. Using the nucleoside diphosphate d(pTp), the formation of T–T base pairs could only be induced via methylation of the phosphate groups. This leads to the suggestion that intermolecular electrostatic phosphate–phosphate repulsion precludes T–T base pairing for unmodified d(pTp). It is shown that T–T pairing is also manifest on the dinucleotide level, provided that the phosphate groups are methylated. Using the dinucleoside phosphate **1** which was separated in its diastereomeric forms, it was shown that the miniduplex melts at $T_m \approx 30$ °C. Furthermore, it was shown that the duplex of **1** is parallel. From the detailed conformational analysis of the individual diastereomers it follows that the duplex has a right-handed helical sense, since the backbone bonds $C_{4'}$–$C_{5'}$ and $C_{5'}$–$O_{5'}$ are preferentially γ^+ and β^t, and the furanoses reside primarily in the south conformation. With the hexamer d(TpTpTpTpTpT), it was shown that T–T pairing also occurs on the hexanucleotide level, after methylation of the phosphate groups. The resulting duplex has a T_m value of approximately 65 °C as was established with UV hyperchromicity and with variable-temperature 500-MHz ^1H NMR. It could be clearly established that the duplex is parallel. Molecular modelling studies on the duplex of phosphate-methylated d(TpTpTpTpTpT) yielded a remarkably slim, parallel structure with about eight residues per turn. The possible relevance of these alternative DNA-like duplexes is briefly mentioned.

Thymine–thymine (T–T) base pairing was recently observed in the crystal structures of 3′,5′-di-*O*-acetylthymidine[1] and *cis*-thymidine-3′,5′-*N*,*N*-dimethylphosphoramidate.[2] Both crystal structures display an approximate twofold rotational symmetry, which is due to the fact that the T-bases are linked via two virtually identical N_3-H···O_4 hydrogen bonds (Figure 1). Following the convention of Rose et al.,[3] it is easily seen that the α faces of the coupled bases are on the same side; i.e., the T-bases are parallel. Therefore, the 5′→3′ vectors run in the same direction on both sides of the T–T pair. The present work is focused on the formation of T–T base pairs in solution. It was found that parallel T–T pairing readily occurs on, e.g., the mono-, di-, and hexanucleotide level, provided that the backbone phosphate groups are triesterified. In a previous communication,[1a] we already published our preliminary results on the phosphate-methylated hexanucleotide duplex. Various physico-chemical techniques (high-resolution proton NMR, UV hyperchromicity) were used in order to characterize these non-Watson–Crick parallel duplexes.

Results and Discussion

T–T Pairing on the Mononucleotide Level. We first studied T–T pairing using the acetylated nucleoside 3′,5′-di-*O*-acetylthymidine[1a] (vide supra) and the nucleoside diphosphate d(pTp). In fact, 3′,5′-di-*O*-acetylthymidine provided the first indication that T–T pairing may occur in aqueous solution, since the imino proton NMR signal was found at a remarkably low-field position (13.45 ppm[4]) in comparison with unlinked thymidine bases (11.2

(1) (a) Koole, L. H.; van Genderen, M. H. P.; Frankena, H.; Kocken, H. J. M.; Kanters, J. A.; Buck, H. M. *Proc. K. Ned. Akad. Wet., Ser. B* **1986**, *89*, 51 (communicated by H. M. Buck at the meeting of Nov 25, 1985). (b) Wilson, C. C.; Low, J. N.; Tollin, P.; Wilson, H. R. *Acta Crystallogr., Sect. C: Cryst. Struct.* **1984**, *40*, 1712.

(2) Bentrude, W. G.; Sopchik, A. E.; Setzer, W. N. *Acta Crystallogr., Sect. C: Cryst. Struct.* **1986**, *42*, 584.

(3) Rose, I. A.; Hanson, K. R.; Wilkinson, K. D.; Wimmer, M. J. *Proc. Natl. Acad. Sci. U.S.A.* **1980**, *77*, 2439.

0002-7863/87/1509-3916$01.50/0